STRUCTURAL SCIENCE
CRYSTAL ENGINEERING
MATERIALS

Volume 76 (2020)

Supporting information for article:

Analysis of charge density in nonaaquagadolinium(III) trifluoromethanesulfonate – insight into Gd^{III}-OH2 bonding

Rafał Janicki and Przemysław Starynowicz

Supplementary information.

Contents

1. Residual densities

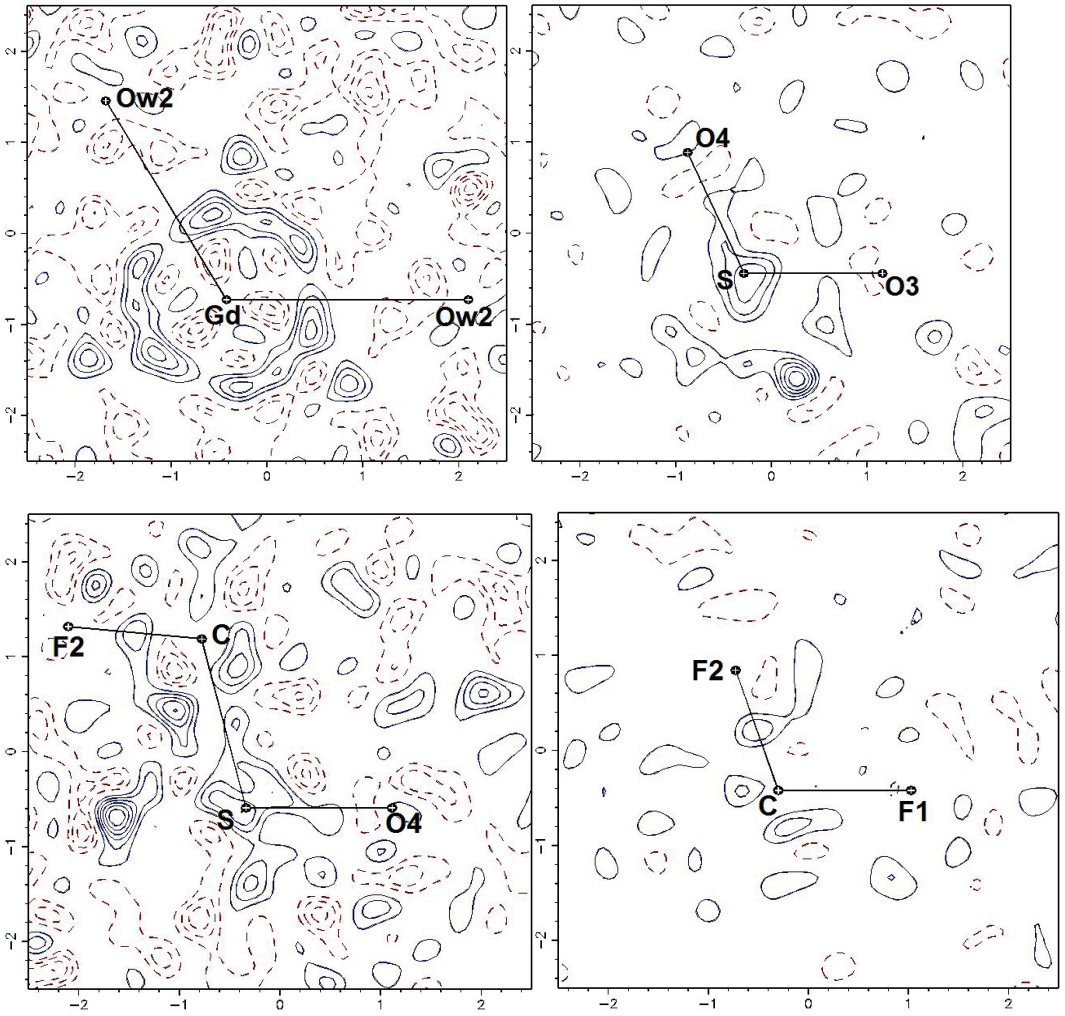

Fig. S1. Residual density maps. The layers are drawn at 0.1 e·Å^{-3}; the positive ones are blue solid, the negative ones – red dashed, the zero layer has been omitted.

2. Some multipole refinement details

The starting configuration of Gd was atom was [Xe]4f^{7}5d6s^{2}, but the wave functions were those calculated for Gd^{3+} plus virtual 5d and 6s. The 5s, 5p, 5d and 6s electrons treated as valence ones (to enable their contraction or expansion).

Table S1. Final parameters of the radial deformation parameters.

atom type	multipole order	a (Å^{-1})	n	κ'	R_{max}(Å)*
Gd	0	20.7870	9	1.008(6)	0.430
	1-4	24.8327	6	1.008(6)	0.240
S	1-2	10.2357	6	1.007(10)	0.582
	3	10.2357	7	1.007(10)	0.679
F	1	9.8001	2	1.3	0.157
	2	9.8001	3	1.3	0.235

	3	9.8001	4	1.3	0.314
O	1	8.4989	2	0.831(12)	0.283
	2	8.4989	3	0.831(12)	0.425
	3	8.4989	4	0.831(12)	0.566
C	1	5.9154	2	0.881(13)	0.383
	2	5.9154	3	0.881(13)	0.576
	3	5.9154	4	0.881(13)	0.768
H	1	3.6196	1	1.2	0.230
	2	3.6196	2	1.2	0.460

* - R_{max} is the position of the respective radial function maximum (from the atom centre).

3. Distances and angles

Table S2**.** Selected geometric parameters (Å, °)

GD—O(W1)	2.4108(3)	F(1)—C	1.3281(11)
GD—O(W2)	2.5208(4)	F(2)—C	1.3331(12)
S—O(3)	1.4488(3)	O(W1)—H(11)	0.99
S—O(4)	1.4515(4)	O(W1)—H(12)	0.99
S—C	1.8329(6)	O(W2)—H(21)	0.99
O(W1)—GD—O(W1)^{ii}	74.432 (8)	O(3)—S—O(4)	113.858 (12)
O(W1)—GD—O(W1)^{iii}	91.404 (11)	O(3)—S—C	104.156 (14)
O(W1)—GD—O(W1)^{iv}	139.123 (4)	O(4)—S—C	103.85 (2)
O(W1)—GD—O(W2)	66.256 (7)	H(11)—O(W1)—H(12)	110.5
O(W1)—GD—O(W2)^{ii}	72.971 (8)	H(21)—O(W2)—H(21)^{iii}	100.6
O(W1)—GD—O(W2)^{v}	134.068 (6)	S—C—F(1)	110.25 (6)
O(W2)—GD—O(W2)^{ii}	120.0	S—C—F(2)	109.52 (6)
O(W2)—GD—O(W2)^{v}	120.0	F(1)—C—F(1)^{i}	109.55 (15)
O(3)—S—O(3)^{i}	115.19 (2)	F(1)—C—F(2)	108.62 (6)

Symmetry codes: (i) *x*, *y*, −*z*+3/2; (ii) −*y*+1, *x*−*y*+1, *z*; (iii) *x*, *y*, −*z*+1/2; (iv) −*y*+1, *x*−*y*+1, −*z*+1/2; (v) −*x*+*y*, −*x*+1, *z*.

4. Hydrogen bonds and F···F contacts

Table S3. Hydrogen bonds

D-H···A	D-H (Å)	H···A (Å)	D···A (Å)	D-H···A (°)
Ow1-H11···O3^{i}	0.99	1.84	2.8123 (4)	166
Ow1-H12···O4	0.99	1.77	2.7491 (4)	170
Ow2-H21···O3^{ii}	0.99	1.93	2.9045 (4)	166

Symmetry codes: ^{i} x-y, x, -1/2+z; ^{ii} –x+y, 1-x, 3/2-z.

Table S4. F···F contacts

F···F contact	F···F (Å)	F···F contact	F···F (Å)
F1···F1^{iii}	2.9103(14)	F1···F2^{iii}	3.0359(16)

Symmetry codes: ^{iii} x-y, x, 1-z.

5. Topology with positions of the bond critical points (bcps)

Table S5. Topological parameters with the positions of bcps.

bond/pair	ρ_c (e.Å^{-3})		$\nabla\rho_c$ (e.Å^{-5})		ellipticity		Position of the bcps		
	exp.	theor.	exp.	theor.	exp.	theor.	R_{ij} (Å)	d_1 (Å)	d_2 (Å)
Gd-Ow1	0.335(4)	0.330	3.561(3)	4.76	0.12	0.09	2.4109	1.2538	1.1571
Gd-Ow2	0.255(2)	0.246	2.843(2)	3.68	0.14	0.11	2.5208	1.3278	1.1930
S-O3	2.15(3)	2.08	-0.41(11)	14.2	0.17	0.06	1.4489	0.5996	0.8493
S-O4	2.19(3)	2.07	-0.30(13)	13.7	0.16	0.07	1.4515	0.5981	0.8534
S-C	1.321(15)	1.34	-6.93(3)	-9.01	0.01	0.00	1.8329	0.9050	0.9279
C-F1	1.976(16)	1.98	-18.28(11)	-11.2	0.06	0.15	1.3284	0.4732	0.8552
C-F2	1.967(20)	1.95	-17.04(11)	-11.0	0.04	0.15	1.3331	0.4782	0.8549
Ow1-H11	2.43(14)	2.31	-42.1(9)	-56.7	0.02	0.02	0.9912	0.7576	0.2336

Ow1-H12	2.33(11)	2.31	-42.3(8)	-56.4	0.04	0.02	0.9906	0.7860	0.2045
Ow2-H21	2.33(7)	2.35	-42.3(5)	-57.6	0.04	0.01	0.9906	0.7605	0.2300
hydrogen bonds									
H11...O3[i]	0.25(5)	0.219	0.59(10)	2.31	0.27	0.01	1.8425	0.6283	1.2142
H12...O4	0.21(4)	0.250	2.28(9)	2.57	0.23	0.01	1.7875	0.6093	1.1782
H21...O3[ii]	0.22(4)	0.171	0.40(7)	1.95	0.16	0.02	1.9630	0.7024	1.2606
F...F contacts									
F1...F1[iii]	0.046(1)	0.034	0.721(1)	0.67	0.29	0.05	2.9127	1.4476	1.4651
F1...F2[iii]	0.033(1)	0.027	0.536(1)	0.50	2.66	0.32	3.0571	1.5076	1.5494

Symmetry codes: [i] x-y, x, -1/2+z; [ii] –x+y, 1-x, 3/2-z; [iii] x-y, x, 1-z.

6. Laplacian maps

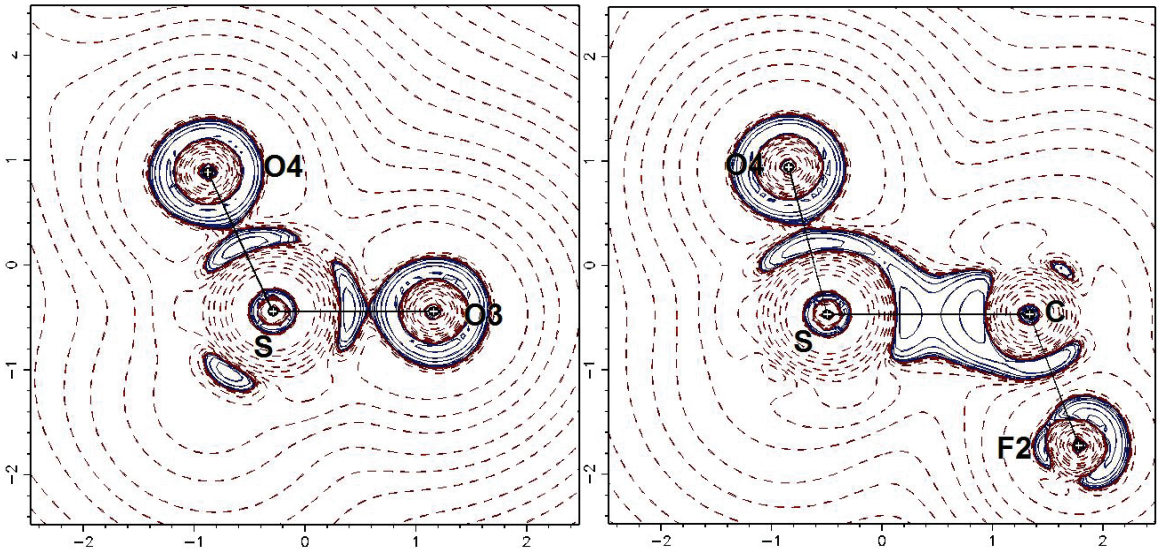

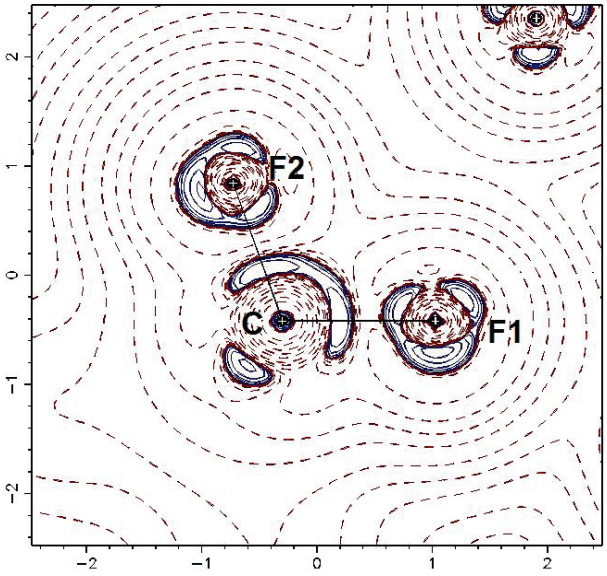

Fig. S2. Laplacian maps, sections through S, O3, O4; O4, S, C; C F1, F2. The contours of negative values are blue solid, the positive –red dashed. The zero contours have been omitted.

7. Description of bonds and contacts not included in the main text

7.1. S-O bonds

The experimental and theoretical charge densities at the critical points of these bonds are in good agreement, but there is a drastic discrepancy between the values of Laplacian. This is a problem that has been repeatedly reported for S-O systems. In the crystal of taurine (Hibbs *et al.*, 2003) the experimental values of $\nabla^2\rho_c$, depending on approach, range between -9.36(5) and 3.17(4) e·Å^{-5}, whereas the theoretical values are 20.2-24.1 e·Å^{-5}. Similar differences (12-27 e·Å^{-5}) were observed for piroxicam and saccharine (Du et al., 2016). They are caused, roughly saying, by small differences of the position of the bond critical point, which, in the case of polarized bonds, is located in the region of rapidly varying Laplacian. A small displacement of the critical point, brought about, among others, by limited flexibility of radial functions used for multipole refinement, may lead thus to sizeable difference between the theoretical $\nabla^2\rho_c$, and that derived from experiment. This question was analyzed thoroughly in the quoted study of taurine and also in other papers (Volkov et al., 2000; Volkov et al., 2001; Starynowicz & Lis, 2014).

7.2. C-S and C-F bonds

There is a fairly good agreement between the experimental and theoretical values of ρ_c and $\nabla^2\rho_c$ for the present C-S bond. This may be regarded as a fortunate outcome, as far as the Laplacian values are concerned. In the case of taurine the experimental and theoretical values were -4.29(3) (model III of the cited work) and -10.2 e·Å^{-5}, respectively. For saccharine the respective values were -5.15 and -11.94 e·Å^{-5}.

Charge density studies for a number of fluoroorganic molecules have been performed and the topological parameters obtained for the C-F bonds show certain variation. In octafluoro-1,2-dimethylenecyclobutane (Lentz et al., 2003) experimental ρ_c values ranged between 2.11(5) and 2.23(4) e·Å^{-3}, with the difference between the *sp*^{2} and *sp*^{3} C atoms being within the experimental error. There were large discrepancies between the experimental and theoretical values of $\nabla^2\rho_c$. For the C(*sp*^{2})F$_2$ groups they were -27.6 – -27.3(3) and -2.7 – -2.8 e·Å^{-5}, whereas for the C(*sp*^{3})F$_2$ ones - -21.1(2) – -20.9(2) and -7.1 e·Å^{-5}, respectively. Similar large discrepancies were reported for fluorinated pyridines (Stammler et al., 2013) (-16.2(1) – -23.4(3) e·Å^{-5} vs. theoretical 1.1 – 3.4 e·Å^{-5}). The experimental densities ranged between 1.92(2) and 2.11(5) e·Å^{-3}. In derivatives of tetrahydroindol-4-one and tetrahydroisoquinoline (Chopra et al., 2006), where fluorine atoms are bonded to phenyl rings, experimental ρ_c and $\nabla^2\rho_c$ were 1.789(18), 1.607(16) e·Å^{-3} and -23.05(8), -7.21(8) e·Å^{-5}, respectively. In pentafluorobenzoic acid (Bach et al., 2001) the experimental densities exceeded 2 e·Å^{-3} and the Laplacians from the multipole refinement were -18.1(1) – -25.7(1) e·Å^{-5}, while the theoretical ones - -0.49 – 0.18 e·Å^{-5}. The quantities reported for 3,3-dimethyl-1-(trifluoromethyl)-1,3-dihydro-1-λ3,2-benziodoxole (Togni reagent; Wang et al., 2018), were 1.83(5)–1.87(5) e·Å^{-3} (ρ_c) and -5.6(3) – -6.8(3) e·Å^{-5}). Our experimental $\nabla^2\rho_c$ values resemble those for C(sp^3)-F bonds in octafluoro-1,2-dimethylenecyclobutane and the theoretical Laplacians differ from the experimental ones not more than 7 e·Å^{-5}.

7.3. O-H bonds

With the exception of Ow1-H11 the charge densities are slightly smaller than those reported for ammonium tetraoxalate dihydrate (Jarzembska et al., 2014). On the other hand, the present values agree with the theoretically computed values, as well as with those reported for $Li_4P_2O_6{\cdot}6H_2O$ (Kinzhybalo et al., 2013). This may be explained by shift of the charge towards the hard cation (Gd^{3+} or Li^+).

7.4. Hydrogen bonds

There is a small discrepancy between the experimental and theoretical values of Laplacian for H11···O3^i and the respective densities for H12···O4 (see Table S5); other quantities are in reasonable agreement. Generally saying, the values resemble other hydrogen bonds formed by water molecules in e.g ammonium tetraoxalate dihydrate (ρ_c between 0.20 and 0.28 e·Å^{-3}, $\nabla^2\rho_c$ between 1.38 and 1.65 e·Å^{-5}) or in tetralithium hypodiphosphate hexahydrate (ρ_c 0.22(3) and 0.26(3) e·Å^{-3}, $\nabla^2\rho_c$ 3.03(5) and 3.34(7) e·Å^{-5}). It should be, however, noticed that the present Laplacian values are rather small.

7.5. F...F contacts

There is extensive literature on weak F···F interactions (e.g. Chopra & Guru Row, 2011) and detailed discussion of this topic is outside the scope of this work, therefore only a few examples may be cited

here. Contacts between 1,4-diiodo-tetrafluorobenzene were characterized by ρ_c 0.034(1) e·Å^{-3} and $\nabla^2\rho_c$ 0.60(1) e·Å^{-5}, in 1,2,3,4,5–pentafluoro–6–{[methoxy(4–methoxyphenyl)methyl] (pentafluorophenyl)phosphoroso}benzene (Karnoukhova et al., 2016) the respective values were: ρ_c 0.016-0.071 e·Å^{-3} and $\nabla^2\rho_c$ 0.23-1.30 e·Å^{-5}. In derivatives of tetrahydroindol-4-one and tetrahydroisoquinoline (Chopra et al., 2006) the critical points between F atoms had ρ_c 0.049 and 0.067 e·Å^{-3}; $\nabla^2\rho_c$ were 1.30 and 0.93 e·Å^{-5}. Our data fit within these values.

8. Fractal dimension and other statistical plots

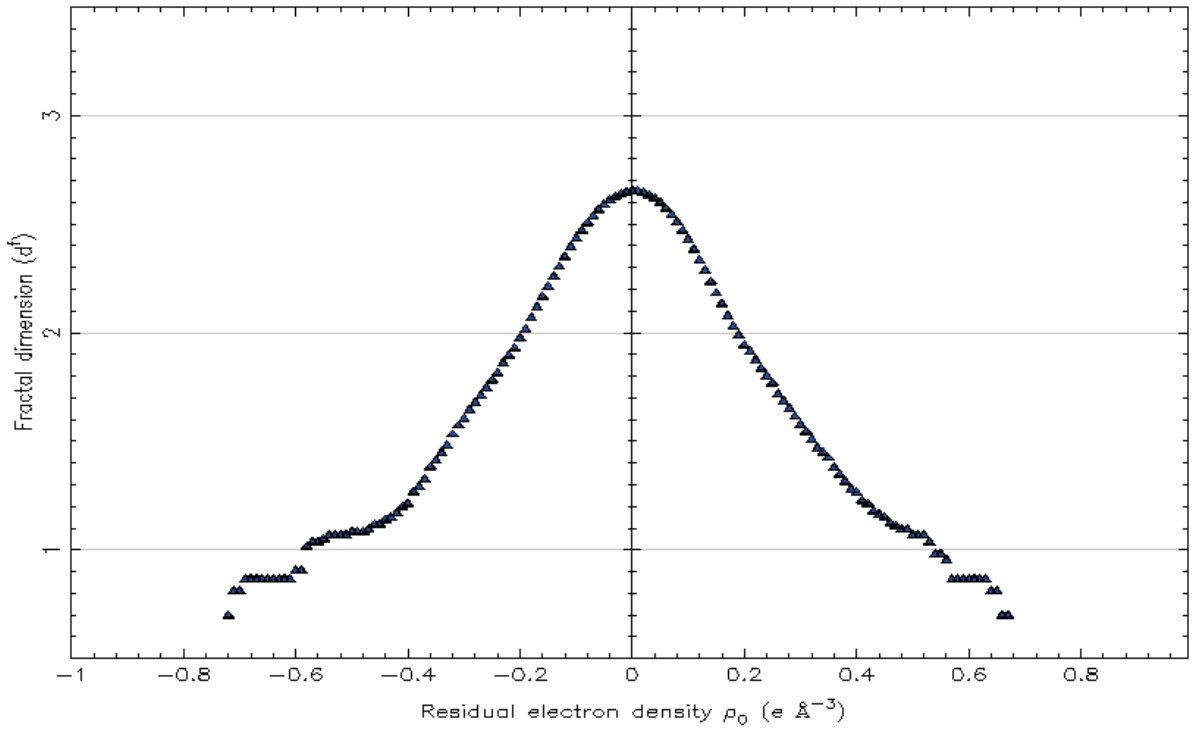

Fig. S3. Fractal dimension plot.

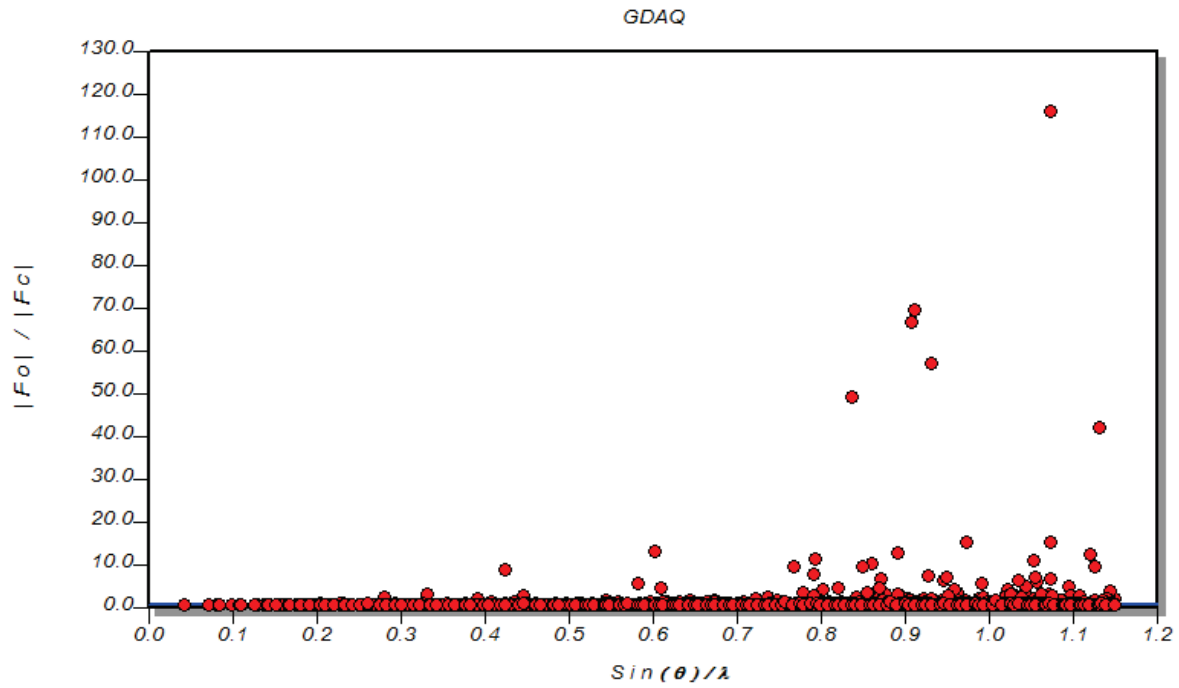

Fig. S4. $|F_0|/|F_c|$ plot.

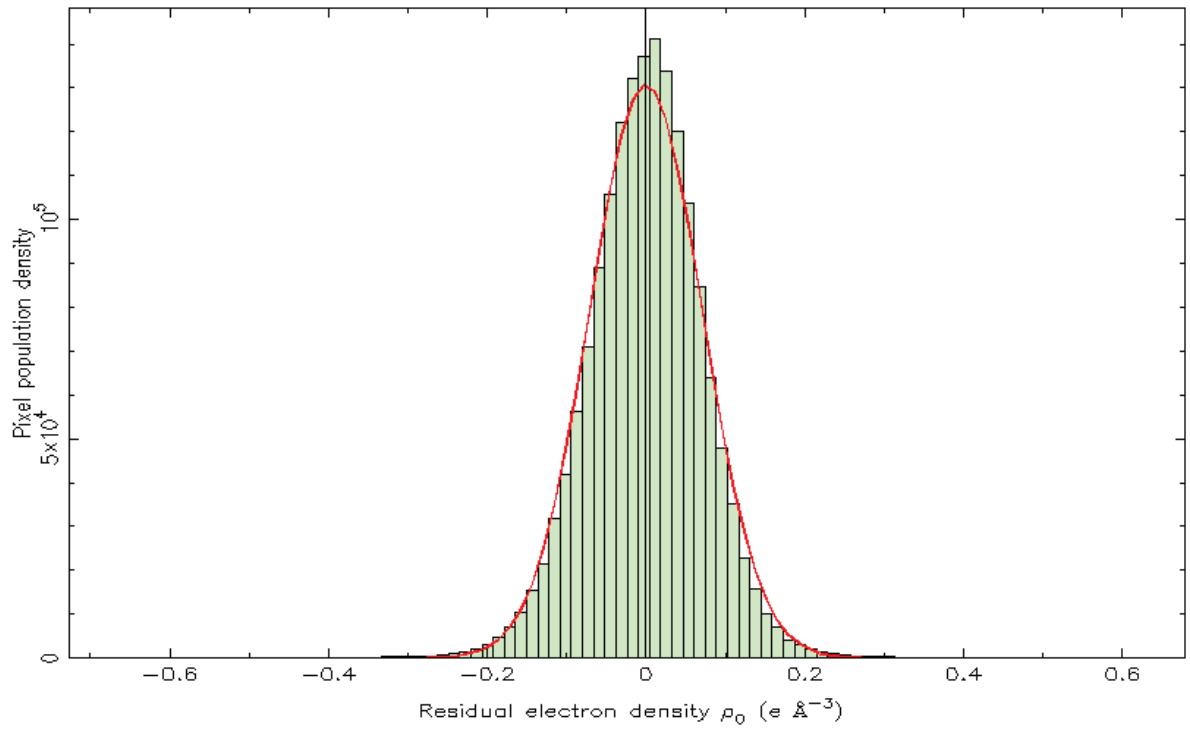

Fig. S5. Residual density distribution.

9. Coordinates of the optimized $[Gd(H_2O)_9]^{3+}$ ion *in vacuo*

Gd	0.01550615	7.94401361	1.82418784
O	-0.77387535	6.20591535	3.41578420
O	1.38395584	8.00898353	3.94362057

O	-0.77388254	9.77504291	3.30725426
O	-0.92309411	9.68189576	0.31765132
O	-0.92275117	6.11859734	0.42432866
O	1.16601329	7.87620509	-0.42008423
O	-2.50400804	7.94773555	1.95103983
O	1.74292501	6.15810976	1.79296974
O	1.74434782	9.72235601	1.68400321
H	-1.27632070	5.39050706	3.22243712
H	-0.58547322	6.17634752	4.37419998
H	2.18073553	7.48230168	4.14941280
H	1.22742363	8.56338354	4.73274462
H	-0.30369050	10.59225842	3.56377012
H	-1.66161630	9.84636539	3.70945694
H	-1.40132878	10.49898885	0.55922136
H	-0.82837530	9.71132728	-0.65449587
H	-1.84648758	6.05099461	0.11275988
H	-0.48362685	5.29979495	0.12189189
H	1.94226563	8.39777925	-0.70288094
H	0.93080380	7.32145830	-1.18916137
H	-3.06602847	7.43427073	2.56347250
H	-3.12384563	8.46235273	1.39827392
H	1.80332168	5.36527401	2.36082433
H	2.47726672	6.07865728	1.15316263
H	2.53693008	9.79778384	2.25061552
H	1.75413265	10.51505528	1.11283608

10. Refinement against full set of data

All the refinement settings were the same except of κ', which were fixed at the values taken from the $\sin(\theta/\lambda)\leq 1.15$ Å^{-1} refinement.

Table S6. Selected refinement details.

$R[F^2 > 3\sigma(F^2)]$, $wR(F^2)$, S; $\sin(\theta/\lambda)\leq 1.15$ Å^{-1}	0.011, 0.026, 1.89
No. of reflections	7951
No. of parameters	203

No. of restraints	1
$\Delta\rho_{max}$, $\Delta\rho_{min}$ (e Å^{-3})	0.90, −0.96

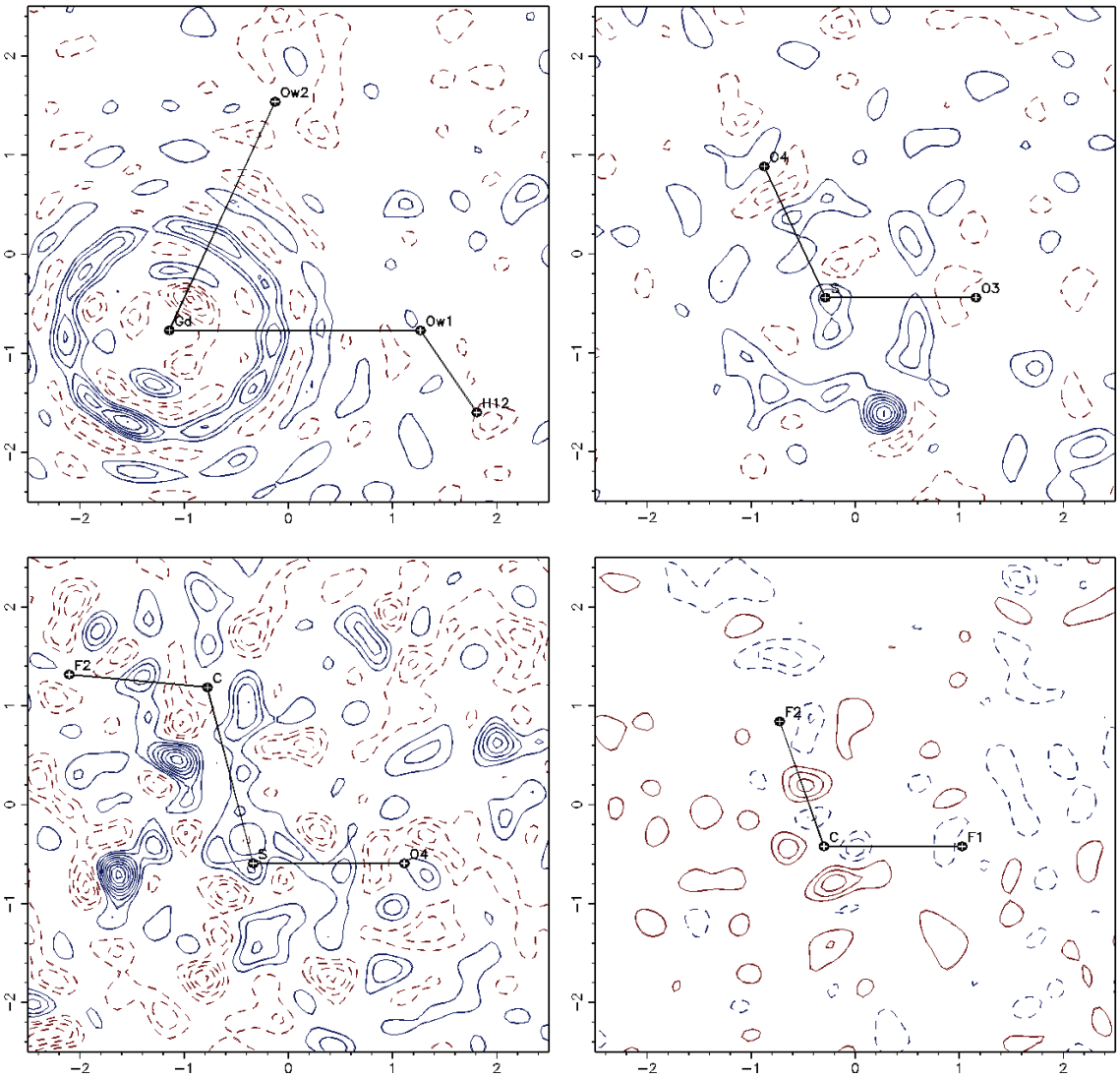

Fig. S6. Residual density maps. The layers are drawn at 0.1 e·Å^{-3}; the positive ones are blue solid, the negative ones – red dashed, the zero layer has been omitted.

Table S7. The Bader charges.

Gd	1.05	S	3.24
F1	-0.66	F2	-0.65
Ow1	-1.31	Ow2	-1.24
O3	-1.14	O4	-1.21

C	1.77	H11	0.66
H12	0.67	H21	0.65

Table S8. Topological parameters.

bond/pair	ρ_c (e.Å^{-3})	$\nabla\rho_c$ (e.Å^{-5})	ellipticity
Gd-Ow1	0.389(4)	4.951(3)	0.13
Gd-Ow2	0.292(2)	3.831(2)	0.14
S-O3	2.091(15)	-0.02(8)	0.16
S-O4	2.16(3)	-1.50(10)	0.15
S-C	1.286(14)	-6.96(35)	0.00
C-F1	1.948(13)	-17.93(9)	0.05
C-F2	1.939(18)	-16.67(9)	0.04
Ow1-H11	2.47(13)	-50.5(9)	0.03
Ow1-H12	2.19(10)	-41.5(8)	0.02
Ow2-H21	2.31(10)	-44.1 (7)	0.03
	hydrogen bonds		
H11...O3^{i}	0.23(4)	0.52(10)	0.33
H12...O4	0.20(4)	2.53 (9)	0.29
H21...O3^{ii}	0.21(4)	0.37(7)	0.13
	F...F contacts		
F1...F1^{iii}	0.041(1)	0.709(1)	0.24
F1...F2^{iii}	0.032(1)	0.533(1)	2.30

Symmetry codes: ^{i} x-y, x, -1/2+z; ^{ii} –x+y, 1-x, 3/2-z; ^{iii} x-y, x, 1-z.

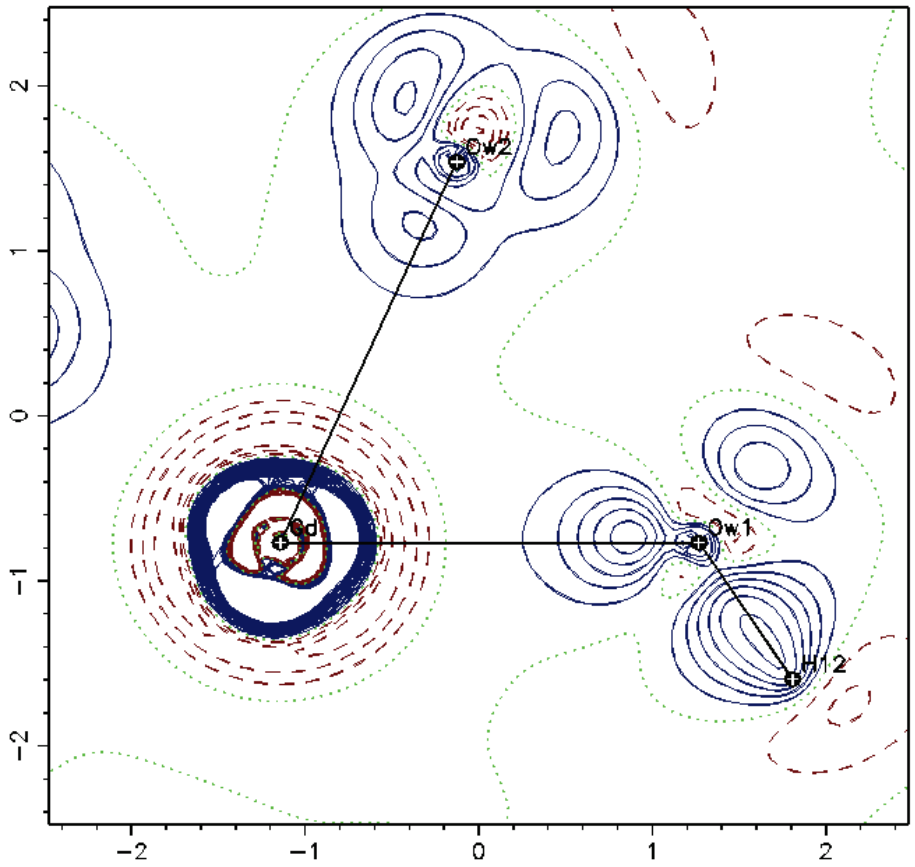

Fig. S7. Deformation density in the plane defined by Gd, Ow1 and Ow2. The contours (positive values – solid, blue; the negative ones – dashed, red; zero –dotted, green) are drawn every 0.1 e·Å^{-3}.

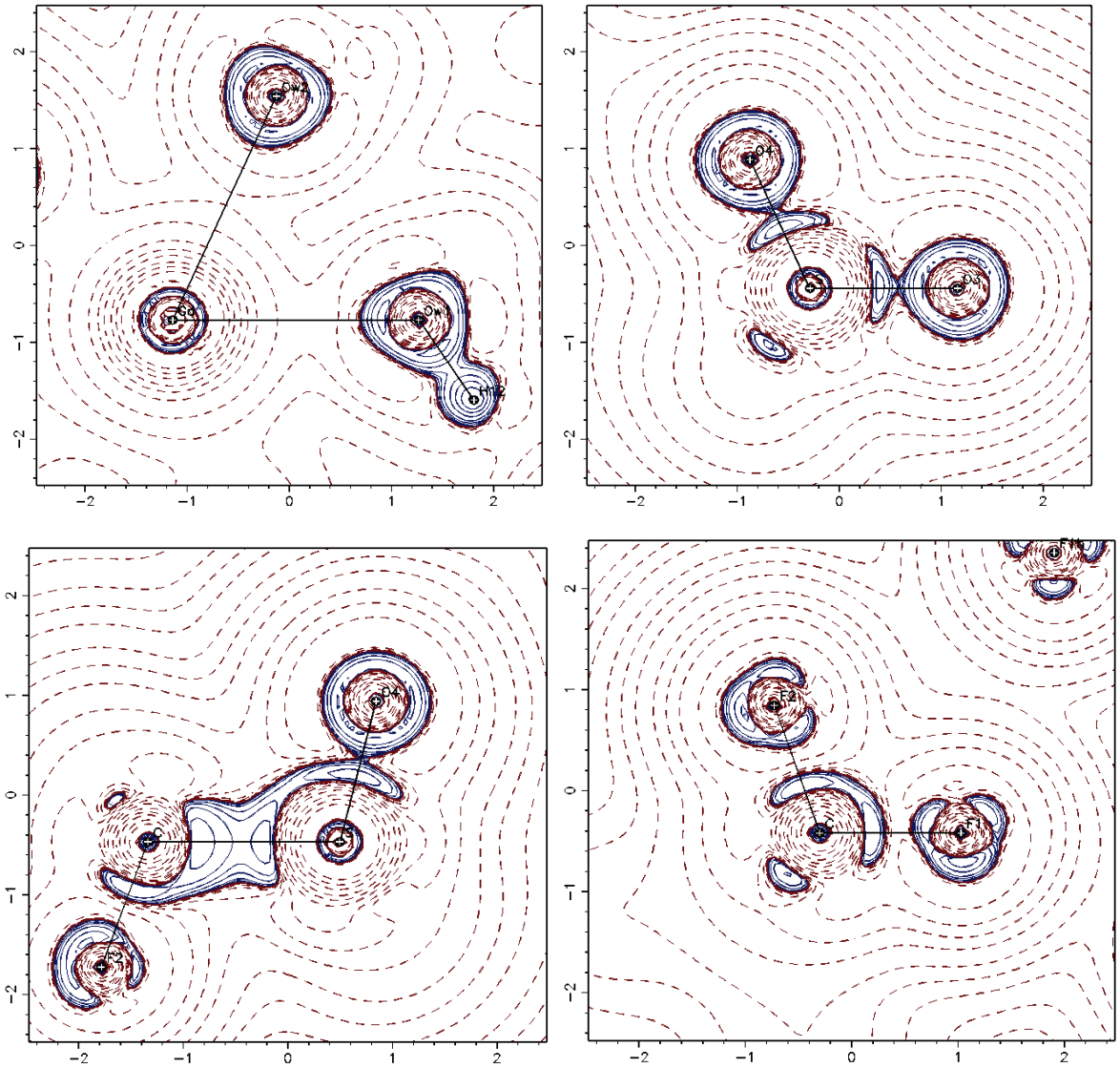

Fig. S8. Laplacian maps, sections through S, O3, O4; O4, S, C; C F1, F2. The contours of negative values are blue solid, the positive –red dashed. The zero contours have been omitted.

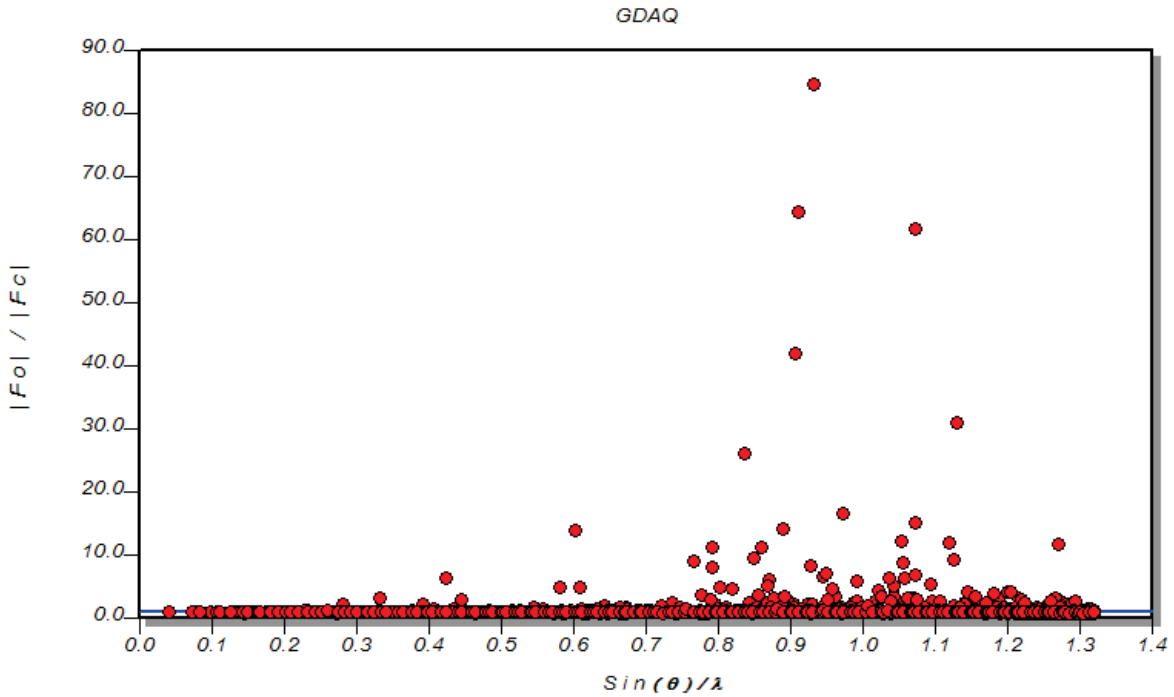

Fig. S9. $|F_0|/|F_c|$ plot.

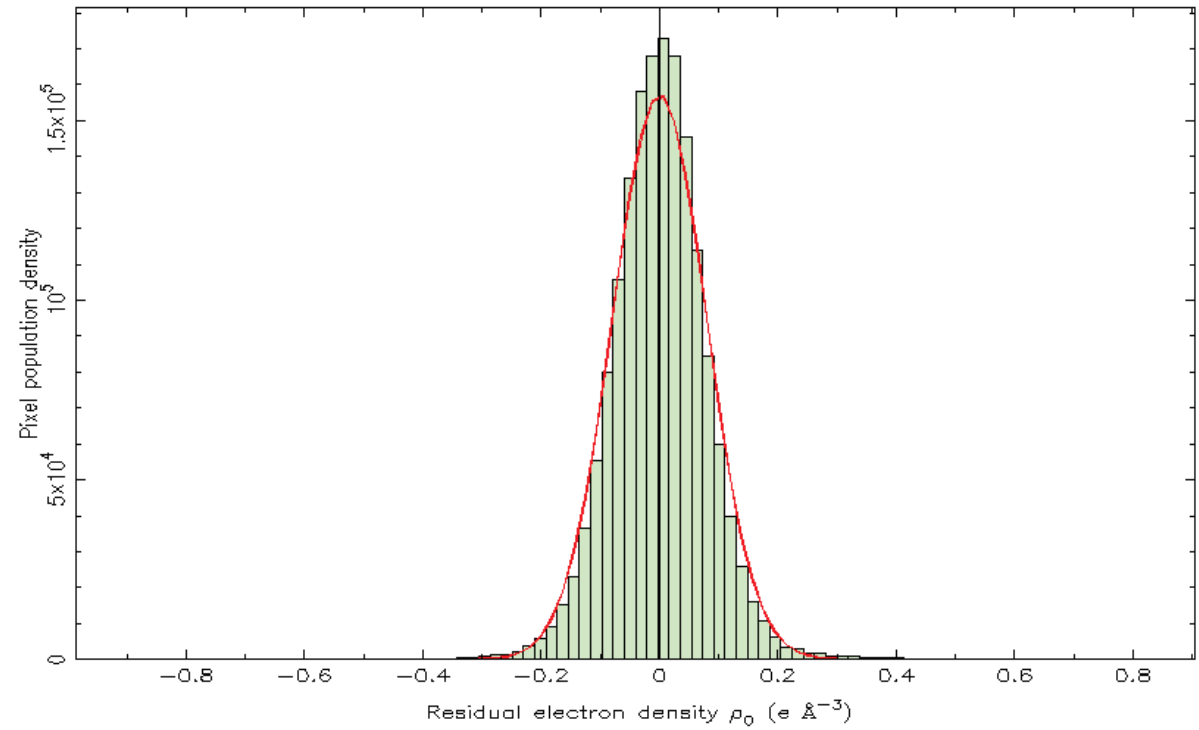

Fig. S10. Residual density distribution.

References

Bach, A., Lentz, D., Luger P. (2001). *J. Phys. Chem. A* **105**, 7405-7412.
Chopra, D., Cameron, T. S., Ferrara, J. D., Guru Row T. N. (2006). *J. Phys. Chem. A* **110**, 10465-10477.
Chopra, D., Guru Row, T. N. (2011). *CrystEngComm* **13**, 2175-2186.

Du, J. J., Váradi, L., Williams, P. A., Groundwater, P. W., Overgaard, J., Platts, J. A., Hibbs, D. E. (2016). *RSC Adv.* **6**, 81578-81590.
Hibbs, D. E., Austin-Woods, C. J., Platts, J. A., Overgaard, J., Turner, P. (2003). *Chem. Eur. J.* **9**, 1075-1084.
Jarzembska, K. N., Kamiński, R., Dobrzycki, Ł., Cyrański, M. K. (2014). *Acta Cryst.*, **B70**, 847–855.
Karnoukhova, V. A., Fedyanin, I. V., Lyssenko, K. A. (2016). *Struct. Chem.* **27**, 17-24.
Kinzhybalo, V., Mermer, A., Lis, T., Starynowicz P. (2013). *Acta Cryst.* **B69**, 344-355.
Lentz, D., Patzschke, M., Bach, A., Scheins, S., Luger, P. (2003). *Org. Biomol. Chem.* **1**, 409-414.
Stammler, H.-G., Vishnevskiy. Yu. V., Sicking, C., Mitzel, N. W. (2013). *CrystEngComm* **15**, 3536-3546.
Starynowicz, P., Lis, T. (2014). *Acta Cryst.* **B70**, 723-731.
Volkov, A., Abramov, Yu., Coppens, P., Gatti, C. (2000). *Acta Cryst.*, **A56**, 332-339.
Volkov, A., Coppens, P. (2001). *Acta Cryst.* **A56**, 395-404.
Wang, R., Kalfa, I., Englert, U. (2018). *RSC Adv*. **8**, 34287-34290.